Energy Savings of Multi-Channel Neurostimulators with Non-Rectangular Current-Mode Stimuli Using Multiple Supply Rails

Kolovou-Kouri, Konstantina; Rashidi, Amin; Varkevisser, Francesc; Serdijn, Wouter A.; Giagka, Vasiliki

Citation (APA)
Kolovou-Kouri, K., Rashidi, A., Varkevisser, F., Serdijn, W. A., & Giagka, V. (2022). Energy Savings of Multi-Channel Neurostimulators with Non-Rectangular Current-Mode Stimuli Using Multiple Supply Rails. In *44th Annual International Conference of the IEEE Engineering in Medicine and Biology Society, EMBC 2022* (pp. 3443-3446). (Proceedings of the Annual International Conference of the IEEE Engineering in Medicine and Biology Society, EMBS; Vol. 2022-July). IEEE. https://doi.org/10.1109/EMBC48229.2022.9871145

Important note
To cite this publication, please use the final published version (if applicable).
Please check the document version above.

Energy Savings of Multi-Channel Neurostimulators with Non-Rectangular Current-Mode Stimuli Using Multiple Supply Rails *

Konstantina Kolovou-Kouri, Amin Rashidi, *Member, IEEE*, Francesc Varkevisser, *Student Member, IEEE*, Wouter A. Serdijn, *Fellow, IEEE* and Vasiliki Giagka, *Member, IEEE*

Abstract—In neuromodulation applications, conventional current mode stimulation is often preferred over its voltage mode equivalent due to its good control of the injected charge. However, it comes at the cost of less energy-efficient output stages. To increase energy efficiency, recent studies have explored non-rectangular stimuli. The current work highlights the importance of an adaptive supply for an output stage with programmable non-rectangular stimuli and accordingly proposes a system-level architecture for multi-channel stimulators. In the proposed architecture, a multi-output DC/DC Converter (DDC) allows each channel to choose among the available supply levels (i.e., DDC outputs) independently and based on its instant voltage/current requirement. A system-level analysis is carried out in Matlab to calculate the possible energy savings of this solution, compared to the conventional approach with a fixed supply. The energy savings have been simulated for a variety of supply levels and waveform amplitudes, suggesting energy savings of up to 83% when employing 6 DDC outputs and the lowest current amplitude explored (250 μA), and as high as 26% for a full-scale amplitude (4 mA).

I. INTRODUCTION

Electrical neural stimulators are an active field of research with applications in treating a wide range of neural disorders (vision and hearing restoration, treatment of pain, or autoimmune conditions via deep brain stimulation (DBS), or vagus nerve stimulation, respectively). To deliver the amount of charge needed for neural activation, neurostimulators typically use either voltage (voltage mode stimulation, VMS) or current (current mode stimulation, CMS) controlled pulses. Although VMS benefits from more energy-efficient architectures, it does not allow for sufficient control of the injected charge given the Electrode-Tissue Interface (ETI) impedance variability. Due to this fact, which impacts safety [1], CMS is preferred in many applications. However, CMS comes at the cost of higher circuit complexity and lower power efficiency at the stimulator output stage, mainly due to the conventional constant supply voltage [2]. The injected current to the tissue is programmed through a current driver powered by this constant supply. This supply should be high enough to fulfill the worst-case scenario, in which the maximum supply level is needed. For scenarios where a smaller supply level would suffice (e.g., the targeted site is easier to activate), any excess voltage drops over the current driver which leads to power dissipation. For multi-channel CMS, in particular, if a single constant supply rail is shared among all channels, all channels with lower supply needs are operated sub-optimally. Furthermore, even within a single channel, in the course of a conventional rectangular stimulus, the required compliance will vary over time due to the capacitive-resistive nature of the ETI. These issues have been addressed in the literature by adjusting the supply voltage to the required voltage compliance at the output stage [3]-[7], [9], or by generating the output current from de-fluxing an inductor without an intermediate voltage [8].

To increase energy efficiency and stimulation efficacy, recent studies have examined the advantages of non-rectangular waveforms [10]. Non-rectangular waveforms (sinusoidal, triangular, Gaussian, rising, and decaying exponential) have exhibited lower energy requirements for tissue activation, making them more energy-efficient compared to the conventional, rectangular type of stimulation. However, a variation on the programmed stimulation current can be translated to variations on the voltage compliance needed at the output stage. Thus, the opportunity to minimize the losses in output stages with non-rectangular waveforms becomes greater, which is often overlooked in the literature.

This paper highlights the importance of employing an adaptive voltage supply to power a stimulation output stage with non-rectangular stimuli. In Section II, different state-of-the-art methods for realizing an adaptive voltage supply are studied to adopt a suitable approach for non-rectangular waveforms. A system-level architecture for a complete implantable device is proposed to visualize the introduced concepts. In Section III, potential energy savings are calculated and validated with top-level simulations. Section IV presents the results for an indicative DBS case study, and Section V concludes the paper.

II. ADAPTIVE SUPPLY RAILS FOR NON-RECTANGULAR STIMULI

An increasing number of studies have proposed different methods for adapting the supply level of a stimulator output stage according to its instant voltage and current requirements, to improve its energy efficiency. Fig. 1 categorizes popular approaches of supply-level adaptation techniques [4]-[9].

One approach is manipulating the wirelessly received AC signal before or while converting it to a DC supply rail (Fig. 1.a&b). As illustrated in Fig. 1.a, [6] directly adjusts the AC power carrier according to the instant requirement of the

K. Kolovou-Kouri, A. Rashidi, F. Varkevisser, W.A. Serdijn and V. Giagka are with the Bioelectronics Section, Dept. of Microelectronics, Faculty of Electrical Engineering, Mathematics and Computer Science, Delft University of Technology, the Netherlands.

K. Kolovou-Kouri and V. Giagka are also with the Technologies for Bioelectronics Group, Dept. of System Integration and Interconnection Technologies, Fraunhofer Institute for Reliability and Microintegration IZM.

W.A. Serdijn is also with the Neuroscience Dept., Erasmus Medical Center, Rotterdam, the Netherlands.
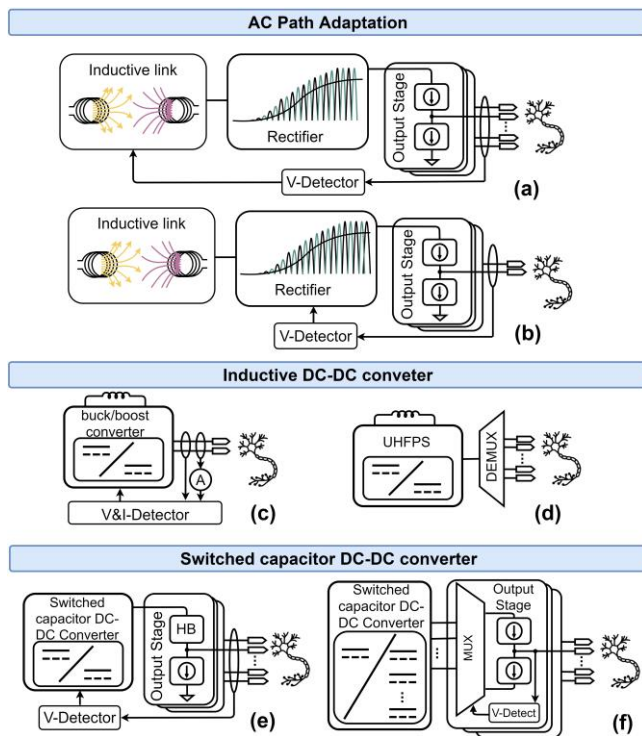(Corresponding author e-mail: K.KolovouKouri@tudelft.nl)

Fig. 1. State of the art supply level adaptation techniques with the point of impact on (a) the wireless link, (b) the rectifier, (c-d) the inductive DC/DC converter, and (e-f) the switched capacitor DC-DC converter. In this figure, HB stands for H-Bridge.

stimulation output stages by informing the external device through uplink data communication. Alternatively, adjusting the rectifier's output voltage according to the required compliance voltage at the output stage is proposed [5]. This approach removes the dependency on uplink communication. However, it leads to a less efficient wireless link as the rectifier will reject part of the transmitted energy to the implant.

A more popular approach is to employ a DC/DC converter at the implant site to generate the adaptive supply rail(s) out of the constant DC voltage generated by either the wireless link interface or a battery [4],[7]-[9]. The proposed DC/DC converters are often based either on inductive buck/boost converters (Fig. 1.c&d) or switch-capacitor charge pumps (Fig. 1.e&f). As illustrated in Fig. 1.c, [7] proposes directly

driving the electrodes with an inductive buck-boost converter and controlling it through closed-loop sensing of the ETI's instant voltage and current. Alternatively, in [8] (Fig. 1.d), an open-loop approach is chosen to charge an inductor with the target current and periodically discharge it to the tissue. While an inductive approach benefits from continuous resolution for generating the voltage and current required at the output stage, it comes at the expense of off-chip inductor(s) and more limited MRI compatibility. Charge pump circuits ([4],[9]) can benefit from fully-integrated architectures but with a limited resolution for the generated adaptive supplies.

Most supply-level adaptation methods support only one channel at a time by generating a single adaptive supply rail, shared between all channels. Thus, in the case of multiple channels demanding different supply levels simultaneously, either the adaptive circuit needs to be duplicated per channel (Fig. 1.c), or the supply rail has to adapt to the highest required level, which would not be optimized for other channels (Fig. 1.a&e). To avoid this, [8] has proposed high-frequency interleaving of ultra-high frequency pulsed stimuli (UHFPS) between multiple channels (Fig. 1.d) at the cost of longer stimulation duration or higher amplitude for the high-frequency pulsed stimuli. Alternatively, a multi-output charge pump has been proposed in [4] (Fig. 1.f), where each channel connects to one of the charge pump outputs based on its instant voltage/current requirement, independent of other channels.

As illustrated in Fig. 2.a, in the case of non-rectangular stimuli, even channels with identical waveforms and identical amplitudes may require different instant currents and, consequently, various instant voltage compliances. Therefore, the method proposed in [4] (Fig. 1.f) is the most suitable approach to be adopted here, as it supports multi-channel operation and does not require off-chip components.

In this paper, based on the system of Fig. 1.f and as a solution against the low efficiency of CMS output stages, a multi-output DC/DC converter that enables adaptive and independent supply rails for multiple stimulation channels with non-rectangular waveform stimuli is proposed. Fig. 2.b demonstrates a generalized architecture of a wireless neurostimulator featuring an energy-efficient output stage with the capability of programming non-rectangular stimulation waveforms. Moving towards battery-less implanted stimulators to reduce their overall size and avoid risky
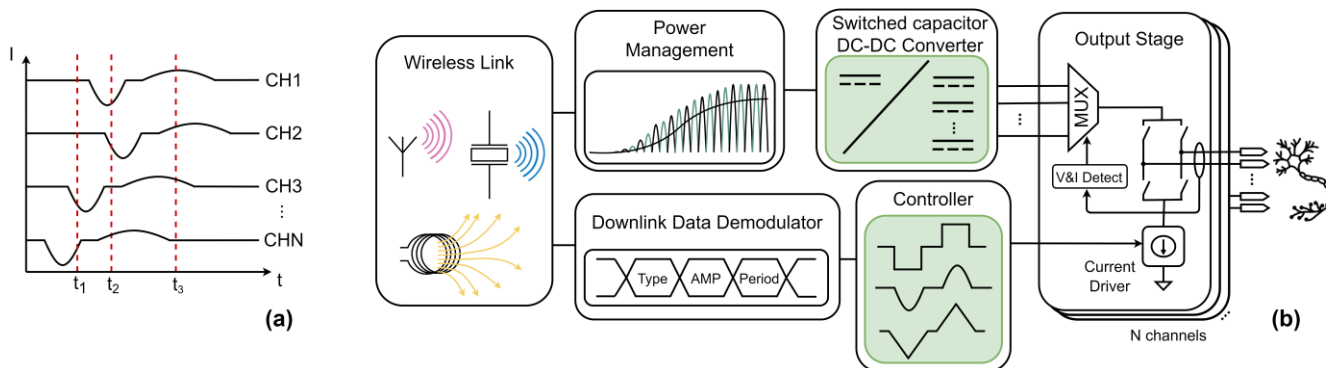

Fig. 2. (a) Illustration of different instant current requirements for different channels at identical waveforms and amplitudes. (b) High-level block diagram of a complete wirelessly-powered implantable device. The wirelessly received power is rectified and received by the proposed switched capacitor DC-DC converter to generate the 6 (depending on the application) DDC outputs to provide for the stimulation output stage. In each output stage, the proper DDC output is chosen using an HV-MUX according to the electrode's monitored voltage and/or current level. Biphasic stimulation is possible with an H-bridge.
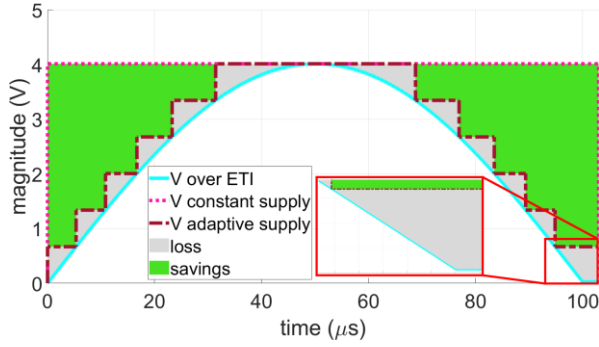
Fig. 3. Voltage over the ETI (RC-load with R_{load}=1kΩ, C_{dl}=10µF) for a half-sine wave at the maximum amplitude (4mA) and the maximum number of available DDC outputs (6), for an adiabatic supply (solid cyan line), for a constant supply (dotted pink line), and for an adaptive supply (dashed purple line). For an amplitude <max, the number of supply rails decreases, thus increasing the system's energy savings.

interventions for a battery replacement, wireless powering of the neurostimulator (using ultrasonic waves, inductive coupling, or RF fields) is preferred in many applications. The received power needs to be rectified and forwarded to a multi-output DC/DC converter for generating and sharing multiple DC supply levels for each channel of the output stage to choose from. To appreciate the design tradeoffs for such a multi-output DC/DC converter architecture, the following sections present a framework that can be used as a guide for designers to study the energy savings for a variety of parameters, and more importantly, the number of supply rails.

III. PROPOSED APPROACH AND VALIDATION METHOD

As mentioned, an adaptive voltage supply at the stimulation output stage can lead to energy savings, especially in the case of a non-rectangular stimulation waveform. Fig. 3 illustrates the benefit of an adaptive supply for a half-sine waveform. Here the voltage supply level is stepped up as soon as the current supply level is not enough for driving the required current and steps down when a smaller supply level suffices. To calculate the energy savings from using an adaptive supply compared to a constant supply, we need to consider the energy (E) required to generate a single pulse over the period T for both cases. This energy is expressed as a function of the power (P) needed to supply said pulse, as

$$E(t) = \int_0^T P(t) \, dt . \qquad (1)$$

For an ideal (also adiabatic [7]) power supply, where the supply follows the needed voltage for stimulation through an infinite amount of supply steps and considering a purely resistive load at the ETI, the power required for one pulse is

$$P(t) = I(t) \cdot V(t) = I^2(t) \cdot R , \qquad (2)$$

where $V = I \cdot R$. However, for a realistic load representation, the capacitive nature of the ETI needs to be considered as well. In this case, the voltage compliance varies according to the capacitive value of the ETI and the injected charge (Q), leading to the following power consumption when assuming a conventional constant voltage supply

$$P_{const}(t) = I(t) \cdot V_{max} , \; V_{max} = \max \left(I(t) \cdot R + \frac{Q(t)}{C} \right) . (3)$$

The effect of the capacitive nature of the ETI is visible at the end of the pulse (Fig. 3, inset). Because of the accumulated charge on the ETI's double-layer capacitor, the voltage does not return to zero. This effect depends strongly on the capacitive value of the ETI, in relation to its real part. In this case, the effect is not that strong, given the chosen values.

In the case of an adaptive power supply, the power is calculated based on the instantaneous voltage needed at the different levels ($V_{quantized}$), as in

$$P_{adapt}(t) = I(t) \cdot V_{quant}(t) = I(t) \cdot \left(I_{quant}(t) \cdot R + \frac{Q(t)}{C} \right) . \quad (4)$$

The energy savings (E_{save}) between the two scenarios (adaptive vs. constant supply) are expressed with a percentage (%) and calculated as

$$E_{save} = (1 - E_{adapt}/E_{const}) \cdot 100\% . \qquad (5)$$

A high-level numerical investigation has been implemented using Matlab to calculate the possible energy savings when comparing an adaptive power supply to the conventional approach. For this analysis, a capacitive-resistive (RC) load of 1 kΩ in series with 10 µF is assumed, based on the typical range of deep brain stimulation (DBS) electrodes used in human patients [11]. Different monophasic stimulation waveforms (half-sine, Gaussian, triangular) are evaluated, with a pulse width of 100 µs, and with stimuli amplitudes from 250 µA to 4 mA, with steps of 250 µA. The energy savings have been calculated for different numbers of equally separated supply rails, ranging from 2 to 6 steps. This provides an insight into the needed number of supply rails and the energy savings for a specific waveform. It should be noted that this calculation acts as a practical example. Adaptation to any impedance and amplitude combination comes with little effort.

IV. RESULTS AND DISCUSSION

Fig. 4 illustrates the power consumption for a constant supply, an adaptive supply with 6 DDC outputs, and an adiabatic supply for the example of a half-sine stimulation pulse while considering the capacitive nature of the ETI (R_{load}=1kΩ, C_{dl}=10µF). In the adiabatic supply case, the voltage supplied is equal to the demand of each stimulus waveform, resulting in very little power loss, coming from the small voltage overhead needed for the current driver. The green shaded area illustrates the energy savings when employing the proposed adaptive supply compared to a conventional constant supply.

Fig. 5 demonstrates the energy savings for a half-sine, with a pulse width of 100 µs, stimuli of different amplitudes, and different numbers of uniformly distributed supply rails. Energy savings of up to 83% are possible when employing 6 supply rails, at the lowest examined amplitude (250 µA). Similar energy savings were calculated for a Gaussian and a triangular waveform, and the results are summarized in Table 1. By decreasing the number of supply rails, the total possible energy savings decrease. This is also the case for larger amplitudes, resulting in a larger needed voltage compliance. For a full-scale (here 4 mA) half-sine, the energy savings reach up to 15%, for a Gaussian up to 22%, and for a triangular waveform up to 26%, when using 6 DDC outputs.
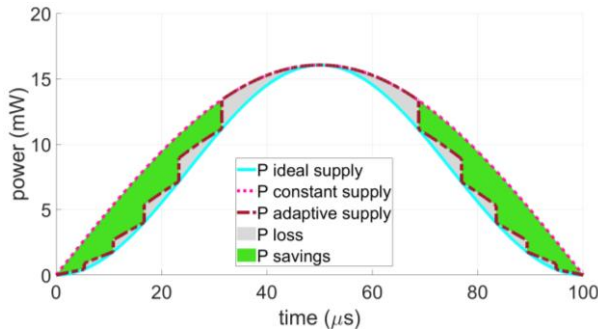
3445

Fig. 4. Power consumption for a half-sine wave (RC-load with R_{load}=1kΩ, C_{dl}=10µF) at the maximum amplitude (4mA) and the maximum number of available DDC outputs (6), for an adiabatic supply (solid cyan line), for a constant supply (dotted pink line), and for an adaptive supply (dashed purple line). The energy savings of the adaptive supply compared to the conventional supply are visualized in green.
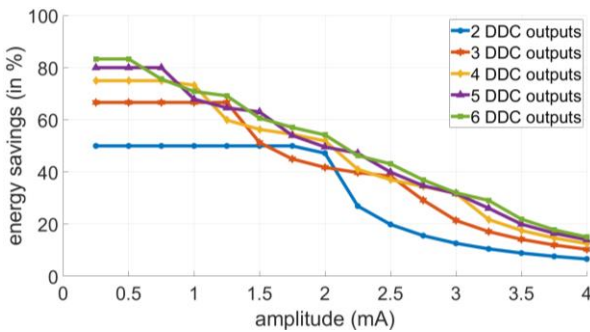

Fig. 5. Energy savings of a half-sine wave (RC-load with R_{load}=1kΩ, C_{dl}=10µF), for stimulus amplitudes varying between 250µA and 4mA, and for 2-6 uniformly distributed DDC outputs. Similar savings can be achieved for the second phase of a biphasic pulse.

The energy savings calculated here are higher for smaller stimulus amplitudes since lower voltage supplies would suffice to generate the pulses. A higher number of supply levels also leads to higher savings. However, the relative increase in energy saving decreases for an increasing number of supply levels. It can be seen from Fig. 5 that the energy savings for 5 and 6 supply rails are comparable. Given the increase in circuit complexity when increasing the number of supply levels, a trade-off can be made between the number of supply rails and the amount of energy saved.

The proposed approach can be advantageous for multi-channel applications with different supply needs for every channel. It allows each stimulation channel to connect to the pre-generated supply rails based on its instant need and independent of other channels. Furthermore, it can benefit multi-channel applications with different electrode sizes at every channel. In such a case, the voltage compliance needs per channel might differ significantly. This approach would allow each stimulation channel to connect to the most suitable pre-generated supply rail.

V. CONCLUSION

This paper presents the possibility of gaining high energy savings for programmable non-rectangular current stimulus waveforms when using an adaptive voltage supply compared to a conventional constant supply. Simulations for the particular indicative case revealed energy savings between

TABLE I. ENERGY SAVINGS VS A CONSTANT SUPPLY IN % FOR DIFFERENT WAVEFORM TYPES, WHEN EMPLOYING 6 DDC OUTPUTS

	Half-Sine		Gaussian		Triangular	
# of DDC outputs	Full scale [a]	Min amp [b]	Full range	Min amp	Full range	Min amp
2	7	50	12	50	13	50
3	10	67	17	67	19	67
4	13	75	20	75	22	75
5	14	80	21	80	24	80
6	15	83	22	83	26	83

a. in the full-scale supply, all 6 DDC outputs are employed

b. min amp is equal to 1/16 of the full-scale supply (250 µA)

7% and 83%, depending on the number of supply levels and stimulus amplitude. The proposed approach offers the potential for full system integration, without off-chip components, for a system aiming at higher overall efficiency and smaller silicon area. Future work will include the design and optimization of the proposed multi-output switched capacitor DC/DC converter, and the implementation of a suitable monitoring and control circuit.

REFERENCES

[1] D. R. Merrill, M. Bikson and J. G. Jefferys, "Electrical stimulation of excitable tissue: Design of efficacious and safe protocols," *J. Neurosci. Methods*, vol. 141, no. 2, pp. 171-198, 2005.

[2] Y. Liu, A. Urso, R. M. Ponte, T. Costa, V. Valente, V. Giagka, W. A. Serdijn, T. G. Constandinou, and T. Denison, "Bidirectional Bioelectronic Interfaces; system design and circuit implications," *IEEE Solid-State Circuits Magazine*, vol. 12, no. 2, pp. 30-46, 2020.

[3] G. E. Ólafsdóttir, W. A. Serdijn, and V. Giagka, "An energy-efficient, inexpensive, spinal cord stimulator with adaptive voltage compliance for freely moving rats," *in Proc. 40th Int. Conf. of the IEEE Engineering in Medicine and Biology (EMBC) 2018*, Honolulu, Hawaii, USA, pp. 2937–40, 2018.

[4] A. Rashidi, N. Yazdani, and A. M. Sodagar, "Fully implantable, multi-channel microstimulator with tracking supply ribbon, multi-output charge pump and energy recovery," *IET Circuits, Devices & Systems*, vol. 15, no. 2, pp. 104–120, 2020.

[5] H.-M. Lee, H. Park, and M. Ghovanloo, "A power-efficient wireless system with adaptive supply control for deep brain stimulation," *IEEE Journal of Solid-state Circuits*, vol. 48, no. 9, pp. 2203–2216, 2013.

[6] E. Noorsal, K. Sooksood, H. Xu, R. Hornig, J. Becker, and M. Ortmanns, "A neural stimulator frontend with high-voltage compliance and programmable pulse shape for epiretinal implants," *IEEE J. Solid State Circuits*, vol. 47, no. 1, pp. 244–256, Jan. 2012.

[7] S. Arfin and R. Sarpeshkar, "An energy-efficient, adiabatic electrode stimulator with inductive energy recycling and feedback current regulation," *IEEE Trans. Biomed. Circuits Syst.*, vol. 6, no. 1, pp. 1–13, Feb. 2012.

[8] A. Urso, V. Giagka, M. van Dongen, and W.A. Serdijn, "An ultra high-frequency 8-channel neurostimulator circuit with 68% peak power efficiency," *IEEE transactions on biomedical circuits and systems*, vol.13. no.5, pp. 882-892, 2019.

[9] I. Williams and T. Constandinou, "An energy-efficient dynamic voltage scaling neural stimulator for a proprioceptive prosthesis," *IEEE Trans. Biomed. Circuits Syst.*, vol. 7, no. 2, pp. 129–139, Apr. 2013.

[10] T. J. Foutz and C. C. McIntyre, "Evaluation of novel stimulus waveforms for deep brain stimulation," *Journal of Neural Engineering*, vol. 7, no. 6, pp. 066008, 2010.

[11] C. R. Butson, C. B. Maks, C. C. McIntyre, "Sources and effects of electrode impedance during deep brain stimulation," *Clin Neurophysiol.*, vol. 117, no. 2, pp. 447-454, 2006.